Chapter 7
Unconventional Elastoplasticity Model: Subloading Surface Model

Elastoplastic constitutive equations with the yield surface enclosing the elastic domain possess many limitations in the description of elastoplastic deformation, as explained in the last chapter. They are called the *conventional model* in the Drucker's (1988) classification of plasticity models. Various *unconventional elastoplasticity* models have been proposed, which are intended to describe the plastic strain rate induced by the rate of stress inside the yield surface. Among them, the subloading surface model is the only pertinent model fulfilling the mechanical requirements for unconventional models. These mechanical requirements are first described and then the subloading surface model is explained in detail.

7.1 Mechanical Requirements

There exist various mechanical requirements, e.g., the thermodynamic restriction and the objectivity for constitutive equations. Among them, the continuity and the smoothness conditions are violated in many elastoplasticity models, while their importance for formulation of constitutive equations has not been sufficiently recognized to date. Before formulation of the plastic strain rate, these conditions will be explained below (Hashiguchi 1993a, b, 1997, 2000).

7.1.1 Continuity Condition

It is observed in experiments that "*stress rate changes continuously for a continuous change of strain rate*". This fact is called the *continuity condition* and is expressed mathematically as follows (Hashiguchi 1993a, b, 1997, 2000).

K. Hashiguchi, *Foundations of Elastoplasticity: Subloading Surface Model*,
DOI 10.1007/978-3-319-48821-9_7

$$\boxed{\lim_{\delta\mathbf{d}\to\mathbf{O}}[\mathring{\boldsymbol{\sigma}}(\boldsymbol{\sigma}, H_i;\ \mathbf{d}+\delta\mathbf{d}) - \mathring{\boldsymbol{\sigma}}(\boldsymbol{\sigma}, H_i;\ \mathbf{d})] \to \mathbf{O}} \tag{7.1}$$

where H_i $(i = 1, 2, 3, \cdots)$ denotes collectively scalar-valued or tensor-valued internal state variables. In addition, $\delta(\ )$ stands for an infinitesimal variation. The response of the stress rate to the input of strain rate in the current state of stress and internal variables is designated by $\mathring{\boldsymbol{\sigma}}(\boldsymbol{\sigma}, H_i;\ \mathbf{d})$. *Uniqueness of solution* is not guaranteed in constitutive equations violating the continuity condition, predicting different stresses or deformations for identical input loading. The violation of this condition is schematically shown in Fig. 7.1. Ordinary elastoplastic constitutive equations, in which the plastic strain rate is derived obeying the consistency condition, fulfill the continuity condition. As described later, however, no elastoplastic constitutive equation fulfills it except for the subloading surface model when they are extended to describe the tangential inelastic strain rate.

The concept of the continuity condition was first advocated by Prager (1949). However, a mathematical expression of this condition was not given. The condition was defined as the continuity of strain rate to the input of stress rate by Prager (1949) inversely to the definition given above. However, identical stress rate directing inwards the yield surface can induce different strain rates in loading and unloading states for softening materials. Also, identical stress rate along the yield surface can induce different strain rates in a perfectly-plastic material as illustrated in Fig. 7.2. Besides, it is noteworthy that a stress rate cannot be given arbitrarily since there exists a limitation in strength of materials although a strain rate can be given arbitrarily. For that reason, the Prager's (1949) notion does not hold in the general loading state including softening and the perfectly plastic states.

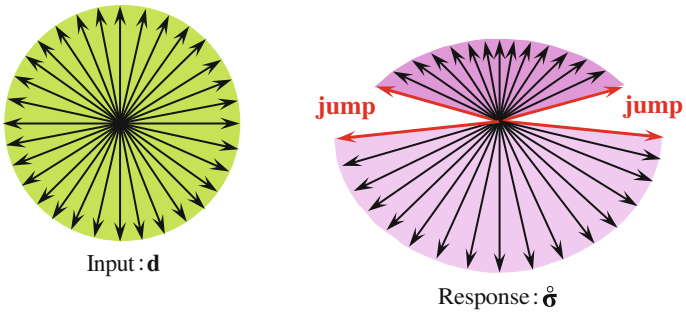

Fig. 7.1 Violation of continuity condition

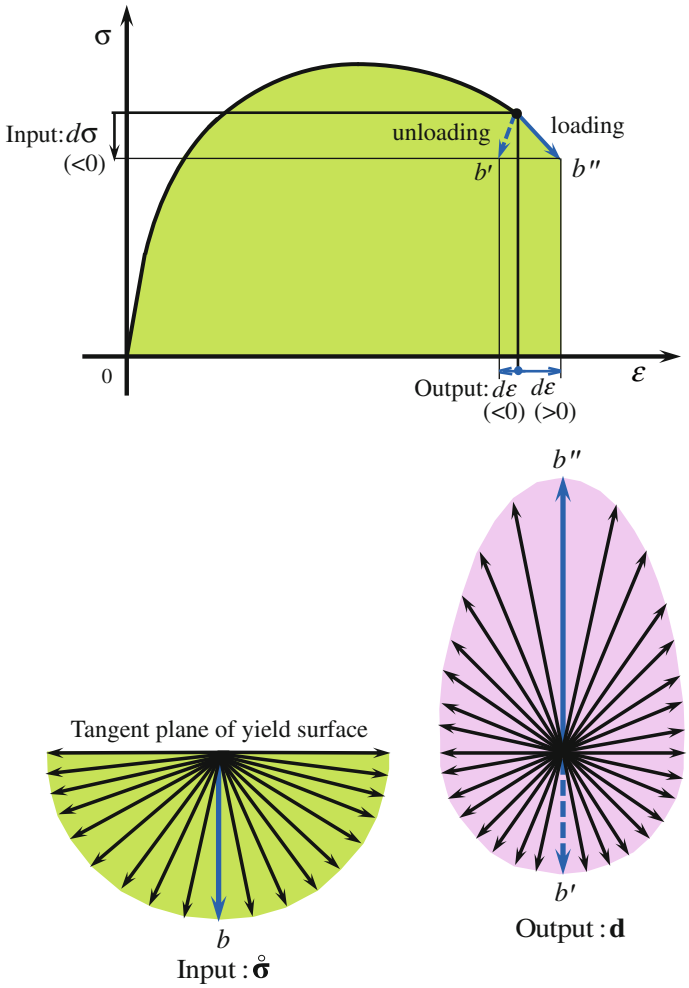

Fig. 7.2 Impertinence of Prager's (1949) continuity condition in softening state

7.1.2 Smoothness Condition

It is observed in experiments that "*the stress rate induced by the identical strain rate changes continuously for a continuous change of stress state*". This fact is called the *smoothness condition* and is expressed mathematically as follows:

$$\lim_{\delta\boldsymbol{\sigma}\to\mathbf{O}} \mathring{\boldsymbol{\sigma}}(\boldsymbol{\sigma} + \delta\boldsymbol{\sigma}, H_i; \mathbf{d}) - \mathring{\boldsymbol{\sigma}}(\boldsymbol{\sigma}, H_i\ ; \mathbf{d}) \to \mathbf{O} \tag{7.2}$$

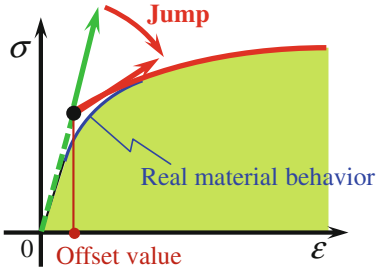

Fig. 7.3 Violation of smoothness condition in the conventional plasticity model and the kinematic hardening cyclic plasticity models assuming a purely elastic domain

A smooth response of stress–strain relation is not described by constitutive equations violating the smoothness condition, causing discontinuous change of tangent modulus, as illustrated in Fig. 7.3 for the conventional elastoplastic constitutive equations assuming the yield surface enclosing a purely-elastic domain. Then, constitutive equations violating the smoothness condition exhibit abrupt change of tangent modulus from the elastic to the elastoplastic state, so that it is required to determine the offset (permanent strain) value, i.e. the plastic stain at yield point, which is accompanied with an arbitrariness (although 0.2 % plastic strain is often used).

The rate-linear constitutive equation is described as

$$\mathring{\boldsymbol{\sigma}} = \mathbf{K}^{ep}(\boldsymbol{\sigma}, H_i) : \mathbf{d} \tag{7.3}$$

where the fourth-order tensor $\mathbf{K}^{ep}$ is the elastoplastic modulus, which is a function of the stress and internal variables, can be described generally as

$$\mathbf{K}^{ep} = \frac{\partial \mathring{\boldsymbol{\sigma}}}{\partial \mathbf{d}} \tag{7.4}$$

Consequently, Eq. (7.2) can be rewritten as

$$\boxed{\lim_{\delta\boldsymbol{\sigma}\to\mathbf{O}} [\mathbf{K}^{ep}(\boldsymbol{\sigma} + \delta\boldsymbol{\sigma}, H_i) - \mathbf{K}^{ep}(\boldsymbol{\sigma}, H_i)] \to \mathbf{O}} \tag{7.5}$$

where $\mathbf{O}$ designates the second-order and fourth-order zero tensors.

Constitutive equations violating the smoothness condition cannot predict a smooth stress-strain curve. Therefore, they cannot describe softening behavior pertinently, as depicted in Fig. 6.13. Further, they cannot predict the strain accumulation for cyclic loading of stress amplitude less than the yield stress, as depicted in Fig. 6.14. The smoothness condition is of great importance in the description of cyclic loading behavior for which an accurate description of plastic strain rate induced by the rate of stress inside the yield surface is required. Among the existing constitutive models only the subloading surface model always fulfills the smoothness condition.

7.2 Subloading Surface (Hashiguchi) Model

The basic concept and equations for the subloading surface model (Hashiguchi and Ueno 1977; Hashiguchi 1978, 1980, 1989) are described below. This is the only model fulfilling the mathematical requirements described in 7.1.

In order to describe the plastic strain rate induced by the rate of stress inside the yield surface, let the following postulate be incorporated based on the concept of the subloading surface (Hashiguchi 1980, 1989, 2013b).

Fundamental postulate of unconventional elastoplasticity (Subloading surface concept): *The stress approaches the yield surface when the plastic strain rate is induced, exhibiting a continuous variation of tangent modulus, but it recedes from the yield surface when only the elastic strain rate is induced.*

In this context, it is first required to incorporate the general measure which describes the approaching degree of the stress to the yield surface, renamed the *normal-yield surface*, in order to formulate the plastic strain rate. Then, let the following ***subloading surface*** which always passes through the current stress and maintains a similar shape and an orientation to the normal-yield surface be introduced (see Fig. 7.4).

$$\boxed{f(\boldsymbol{\sigma}) = RF(H)} \tag{7.6}$$

where $R(0 \leq R \leq 1)$ is the ratio of the size of the subloading surface to that of the normal-yield surface and called the *normal-yield ratio*, playing the role for the measure of approaching degree to the normal-yield surface.

Based on the above-mentioned fundamental postulate of elastoplasticity, the rate of the normal-yield ratio must satisfy the following conditions (see Fig. 7.5).

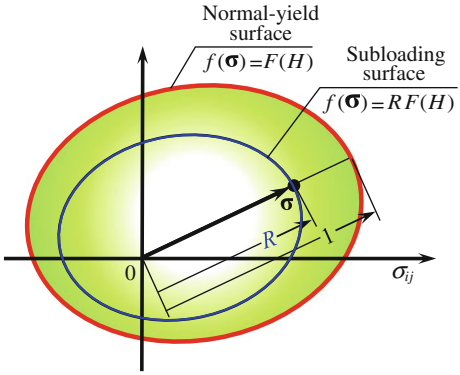

Fig. 7.4 Normal-yield and subloading surfaces

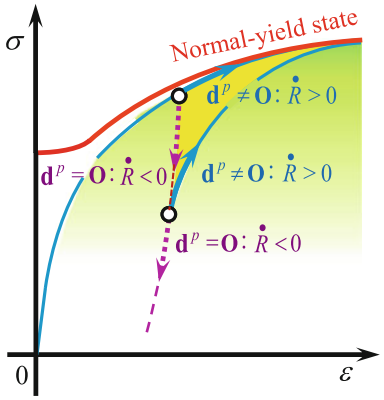

Fig. 7.5 Plastic strain rate based on the subloading surface concept

$$\dot{R}\begin{cases} \to \infty \text{ for } R = 0 \\ > 0 \text{ for } R < 1 \\ = 0 \text{ for } R = 1 \\ (< 0 \text{ for } R > 1) \end{cases} \quad \text{for } \mathbf{d}^p \neq \mathbf{O} \tag{7.7}$$

$$\dot{R}\begin{cases} = 0 \text{ for } \mathbf{d}^e = \mathbf{O} \\ < 0 \text{ for } \mathbf{d}^e \neq \mathbf{O} \end{cases} \quad \text{for } \mathbf{d}^p = \mathbf{O} \tag{7.8}$$

Here, the rate of the normal-yield ratio evolves with the plastic strain rate, obeying Eq. (7.7) but it is calculated from the equation of the subloading surface in Eq. (7.6), substituting a stress changing by the elastic constitutive relation under fixed internal variables when only the elastic strain rate is induced. Then, it follows that

$$\boxed{\dot{R} = U(R)||\mathbf{d}^p|| = U(R)\dot{\lambda} \quad \text{for} \quad \mathbf{d}^p \neq \mathbf{O}} \tag{7.9}$$

$$R = \frac{f(\boldsymbol{\sigma})}{F} \quad \text{for} \quad \mathbf{d}^e \neq \mathbf{O}, \mathbf{d}^p = \mathbf{O} \tag{7.10}$$

where $U(R)$ is the monotonically-decreasing function of R fulfilling the conditions (see Fig. 7.6).

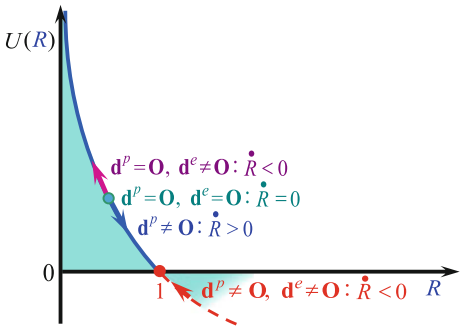

Fig. 7.6 Function $U(R)$ in rate of normal-yield ratio R

$$U(R)\begin{cases} \to\ +\infty \text{ for } R=0 \text{ (elastic state)} \\ >0 \text{ for } R<1 \text{ (subyield state)} \\ =0 \text{ for } R=1 \text{ (normal-yield state)} \\ <0 \text{ for } R>1 \text{ (over normal-yield state)} \end{cases} \tag{7.11}$$

The function $U(R)$ in Eq. (7.9) with Eq. (7.11) is schematically shown in Fig. 7.6.

The explicit form of the function $U(R)$ is given by

$$U(R)=u\cot[(\pi/2)R] \tag{7.12}$$

and the other examples of the function $U(R)$ are shown as

$$U(R)=-u\ln R,\ U(R)=u\left(\frac{1}{R}-1\right) \tag{7.13}$$

where u is the material parameters. Here, note that the normal-yield ratio R increases obeying the evolution rule in Eq. (7.9) formulated by the plastic strain rate in the plastic-loading process. On the other hand, it decreases obeying Eq. (7.10) where R is calculated using the stress calculated by the elastic constitutive relation in Eq. (6.29) in the elastic-unloading process, where the internal variable F is fixed.

Equation (7.9) with Eqs. (7.12) and (7.13) is analytically integrated as follows:

$$\left.\begin{array}{ll} R=\dfrac{2}{\pi}\cos^{-1}\left(\cos\left\{\dfrac{2}{\pi}R_0\exp\left[-\dfrac{2}{\pi}u(\varepsilon^p-\varepsilon_0^p)\right]\right\}\right) & \text{for } U=u\cot\left(\dfrac{2}{\pi}R\right) \\ R(\ln R-1)-R_0(\ln R_0-1)=u(\varepsilon^p-\varepsilon_0^p) & \text{for } U=-u\ln R \\ -R(\ln R+1)+R_0(\ln R_0+1)=u(\varepsilon^p-\varepsilon_0^p) & \text{for } U=u\left(\dfrac{1}{R}-1\right) \end{array}\right\} \tag{7.14}$$

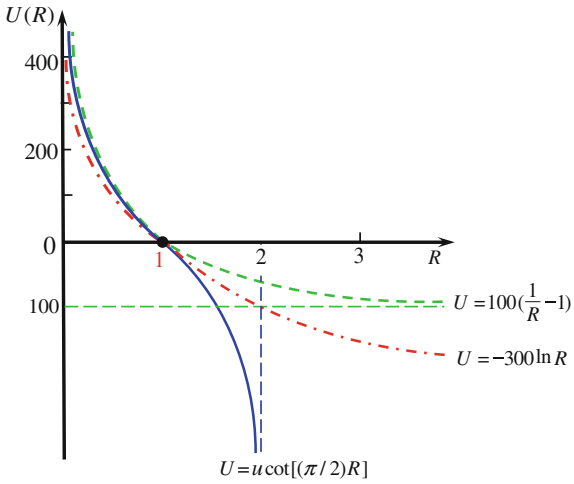

Fig. 7.7 Three types of function $U(R)$ in the evolution rule of the normal friction-yield ratio R

under the initial condition $\varepsilon^p = \varepsilon_0^p : R = R_0$, where $\varepsilon^p \equiv \int ||\mathbf{d}^p|| dt (t : \text{ time})$. Here, note that analytical expression of R holds only for the cotangent function in Eq. (7.14)$_1$, although inversely ε^p can be expressed analytically by R for all of these functions.

Further, note that the following inequality holds as depicted in Fig. 7.7 in which $u = 30$ is used for $u\cot[(\pi/2)R]$ and $u[(1/R) - 1]$ and $u = 100$ for $-u\ln R$.

$$u\ \cot[(\pi/2)R] < -u\ \ln R < u(\frac{1}{R} - 1) < 0 \quad \text{For } R > 1 \tag{7.15}$$

when the material parameter u is chosen such that the values of $U(R)$ in these functions are almost identical in the range $R < 1$, noting

$$\left.\begin{aligned} R \to 2 : \quad & \dot{R} \to -\infty \text{ for } U = u\ \cot[(\pi/2)R] \\ R \to \infty : \quad & \dot{R} \to -\infty \text{ for } U = -\mathrm{u}\ \ln R \\ R \to \infty : \quad & \dot{R} \to -u \quad \text{for } U = u\left(\frac{1}{R} - 1\right) \end{aligned}\right\} \tag{7.16}$$

The cotangent function in Eq. (7.12) would be most beneficial among the three functions shown above by the following reasons.

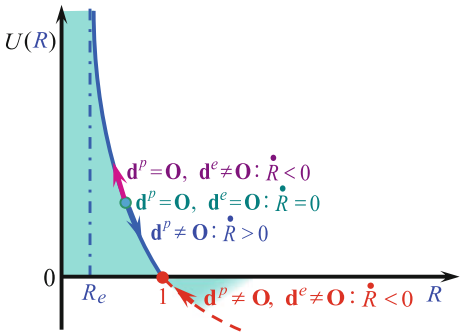

Fig. 7.8 Function $U(R)$ with purely-elastic domain for evolution rule of normal-yield ratio

(1) The analytical expression of R can be obtained only for the cotangent function in Eq. (7.12) as shown in Eq. $(7.14)_1$.
(2) It possesses the largest negative value in the range $R > 1$ among these three kinds of function $U(R)$. Then, it provides the most intense controlling function to pull back the stress to the normal-yield surface when the stress jumps out from that surface in numerical calculations as will be explained in Sect. 7.3 with Fig. 7.13.

Here, note that there exist a lot of materials containing usual metals in which the plastic strain rate is hardly induced in a wide range of the normal-yield ratio. Then, let the following relation be assumed instead of Eq. (7.11), in which the plastic strain rate is not induced until the normal-yield ratio R reaches a certain value of the material parameter $R_e(<1)$ (see Fig. 7.8).

$$U(R)\begin{cases} \to\ +\infty \text{ for } 0\le R\le R_e \text{ (elastic state)} \\ >0 \text{ for } R_e<R\ <1 \text{ (subyield state)} \\ =0 \text{ for } R\ =1 \text{ (normal-yield state)} \\ <0 \text{ for } R\ >1 \text{ (over normal-yield state)} \end{cases} \tag{7.17}$$

The material parameter R_e is interpreted to be the ratio of the (half) stress amplitude σ_{fl} at the fatigue (or endurance) limit, i.e. the fatigue limit stress to the yield stress σ_y under the zero value of average stress $\bar{\sigma}$, i.e. $R_e = \sigma_{fl}/\sigma_y|_{\bar{\sigma}=0}$. Fatigue limit is observed in steels, titanium, etc. but it is not observed in other materials involving non-ferrous metals.

Note here that the incorporation of the material parameter R_e does not mean the incorporation of the yield surface enclosing a purely-elastic domain as known from the fact: The plastic strain rate is predicted for the cyclic loading with a small stress amplitude under a high average stress by the subloading surface model with the incorporation of R_e but it cannot be predicted if the yield surface enclosing a purely-elastic domain is incorporated as seen in the cyclic kinematic hardening model, i.e. the multi surface, the two surface and the superposed kinematic hardening models which will be described in Sect. 8.2.

Equation (7.12) is modified to satisfy Eq. (7.17) as follows:

$$U(R) = u \cot\left(\frac{\pi}{2}\frac{\langle R - R_e\rangle}{1 - R_e}\right) \tag{7.18}$$

where $\langle\ \rangle$ is the Macaulay's bracket defined by $\langle s\rangle = (s + |s|)/2$, i.e. $s < 0 : \langle s\rangle = 0$ and $s \geq 0 : \langle s\rangle = s$ (s: arbitrary scalar variable). Equation (7.18) conforms to the fulfillment of the smoothness condition since it decreases continuously from infinite value in $R = R_e$. If u is fixed to be constant, Eq. (7.9) with Eq. (7.18) can be integrated analytically as

$$\left.\begin{aligned} R &= \frac{2}{\pi}(1 - R_e)\cos^{-1}\left[\cos\left(\frac{\pi}{2}\frac{R_0 - R_e}{1 - R_e}\right)\exp\left(-u\frac{\pi}{2}\frac{\varepsilon^p - \varepsilon_0^p}{1 - R_e}\right)\right] + R_e \\ \varepsilon^p - \varepsilon_0^p &= \frac{2}{\pi}\frac{1 - R_e}{u}\ln\frac{\cos\left(\frac{\pi}{2}\frac{R_0 - R_e}{1 - R_e}\right)}{\cos\left(\frac{\pi}{2}\frac{R - R_e}{1 - R_e}\right)} \end{aligned}\right\} \text{for } R_0 \geq R_e \tag{7.19}$$

whilst one must set $R_0 = R_e$ for $R_0 < R_e$. However, the judgment whether of $R < R_e$ or $R \geq R_e$ is required in Eq. (7.18). The judgment whether R reaches R_e is required in Eq. (7.18), although the yield judgment is not required.

Equation (7.18) with the purely-elastic limit R_e is given above. However, a monotonic loading behaviour and a low cycle loading behavior with a large stress amplitude cannot be realistically described resulting in an excessively large plastic strain accumulation if we choose $R_e \cong 0$ and a high cycle loading behaviour with a small stress amplitude cannot be described resulting in no accumulation of plastic strain if we choose $R_e \gg 0$. Therefore, Eq. (7.18) is not applicable to a general cyclic loading behaviour with variable (fluctuating) stress amplitudes.

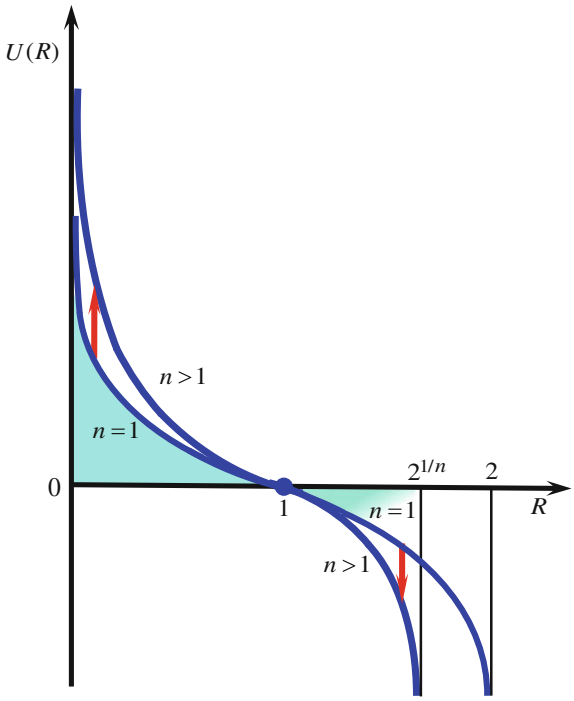

Fig. 7.9 Extended function $U(R) = u\ \cot[(\pi/2)R^n]$

Eventually, any of Eqs. (7.12), (7.13) and (7.18) is inapplicable to the prediction of cyclic loading behavior under variable stress amplitudes in materials without a fatigue limit. The following functions would be applicable to general cyclic loading behavior in wide classes of materials.

$$U(R) = u\cot\left(\frac{\pi}{2}\left\langle\frac{R-R_e}{1-R_e}\right\rangle^n\right) \tag{7.20}$$

$$U(R) = u\left(\left\langle\frac{1-R_e}{R-R_e}\right\rangle^n - 1\right) \tag{7.21}$$

where $n(\geq 1)$ is the material parameter. The value of the function $U(R)$ is larger throughout a whole region of R for a lager value of u, and it is larger in a region of

small value of R for a larger value of n. The function in Eq. (7.12) is schematically illustrated in Fig. 7.9 for $R_e = 0$.

The time-differentiation of Eq. (7.6) of the subloading surface leads to

$$\frac{\partial f(\boldsymbol{\sigma})}{\partial \boldsymbol{\sigma}} : \mathring{\boldsymbol{\sigma}} - R\dot{F} - \dot{R}F = 0 \tag{7.22}$$

Substituting Eq. (7.6) into Eq. (6.32), one has

$$\frac{\partial f(\boldsymbol{\sigma})}{\partial \boldsymbol{\sigma}} : \boldsymbol{\sigma} = RF \tag{7.23}$$

which yields

$$\mathbf{n} : \boldsymbol{\sigma} = \frac{\frac{\partial f(\boldsymbol{\sigma})}{\partial \boldsymbol{\sigma}} : \boldsymbol{\sigma}}{\left\| \frac{\partial f(\boldsymbol{\sigma})}{\partial \boldsymbol{\sigma}} \right\|} = \frac{RF}{\left\| \frac{\partial f(\boldsymbol{\sigma})}{\partial \boldsymbol{\sigma}} \right\|}, \frac{1}{\left\| \frac{\partial f(\boldsymbol{\sigma})}{\partial \boldsymbol{\sigma}} \right\|} = \frac{\mathbf{n} : \boldsymbol{\sigma}}{RF} \tag{7.24}$$

where

$$\mathbf{n} \equiv \frac{\partial f(\boldsymbol{\sigma})}{\partial \boldsymbol{\sigma}} / \left\| \frac{\partial f(\boldsymbol{\sigma})}{\partial \boldsymbol{\sigma}} \right\| \left(\|\mathbf{n}\| = 1 \right) \tag{7.25}$$

Equation (7.22) with Eq. (7.24) results in

$$\mathbf{n} : \left[\mathring{\boldsymbol{\sigma}} - \left(\frac{\dot{F}}{F} + \frac{\dot{R}}{R} \right) \boldsymbol{\sigma} \right] = 0 \tag{7.26}$$

Now, adopt the associated flow rule

$$\mathbf{d}^p = \dot{\lambda}\, \mathbf{n} \; \left(\dot{\lambda} = \|\mathbf{d}^p\| > 0 \right) \tag{7.27}$$

The evolution rule of the normal-yield ratio is described as the equation $\dot{R} = U(R)\dot{\lambda}$ in addition to the Eq. (7.9) for the expression of the flow rule in Eq. (7.27). Note, however, that the equation $\dot{R} = U(R)\dot{\lambda}$ does not hold for the expression of the flow rule $\mathbf{d}^p = \dot{\lambda}\, \partial f(\boldsymbol{\sigma})/\partial \boldsymbol{\sigma}$ because of $\|\partial f(\boldsymbol{\sigma})/\partial \boldsymbol{\sigma}\| \neq 1$ in general.

Substituting Eqs. (6.42) and $(7.9)_1$ with Eq. (7.27), one has

$$\mathbf{n}:\left[\mathring{\boldsymbol{\sigma}}-\left(\frac{F'}{F}f_{Hn}(\boldsymbol{\sigma},H;\mathbf{n})\dot{\bar{\lambda}}\ +\ \frac{U(R)}{R}\dot{\bar{\lambda}}\right)\boldsymbol{\sigma}\right]=0 \tag{7.28}$$

It follows from Eqs. (7.27) and (7.28) that

$$\dot{\bar{\lambda}}=\frac{\mathbf{n}:\mathring{\boldsymbol{\sigma}}}{\bar{M}^p},\ \mathbf{d}^p=\frac{\mathbf{n}:\mathring{\boldsymbol{\sigma}}}{\bar{M}^p}\mathbf{n} \tag{7.29}$$

where

$$\boxed{\bar{M}^p\equiv\left(\frac{F'}{F}f_{Hn}(\boldsymbol{\sigma},H;\mathbf{n})+\frac{U(R)}{R}\right)\mathbf{n}:\boldsymbol{\sigma}} \tag{7.30}$$

which is reduced to the plastic modulus of the conventional elastoplasticity, i.e.

$$\bar{M}^p=\frac{F'}{F}f_{Hn}(\boldsymbol{\sigma},H;\mathbf{n})\mathbf{n}:\boldsymbol{\sigma}=M^p \tag{7.31}$$

in the normal-yield state $(R=1\rightarrow U(R)=0)$.

The strain rate is described from Eqs. $(6.27)_1$, (6.29) and (7.29) as

$$\boxed{\mathbf{d}=\mathbf{E}^{-1}:\mathring{\boldsymbol{\sigma}}+\frac{\mathbf{n}:\mathring{\boldsymbol{\sigma}}}{\bar{M}^p}\mathbf{n}=\left(\mathbf{E}^{-1}\ +\ \frac{\mathbf{n}\otimes\mathbf{n}}{\bar{M}^p}\right):\mathring{\boldsymbol{\sigma}}} \tag{7.32}$$

from which the magnitude of plastic strain $\dot{\bar{\lambda}}$ in terms of strain rate, denoted by the symbol $\dot{\Lambda}$, is derived as follows:

$$\dot{\Lambda}\ =\ \frac{\mathbf{n}:\mathbf{E}:\mathbf{d}}{\bar{M}^p+\mathbf{n}:\mathbf{E}:\mathbf{n}},\ \mathbf{d}^p=\frac{\mathbf{n}:\mathbf{E}:\mathbf{d}}{\bar{M}^p+\mathbf{n}:\mathbf{E}:\mathbf{n}}\mathbf{n} \tag{7.33}$$

The stress rate is described from Eq. (6.29) with Eq. (7.33) as

$$\boxed{\mathring{\boldsymbol{\sigma}}\ =\mathbf{E}:\mathbf{d}-\frac{\mathbf{n}:\mathbf{E}:\mathbf{d}}{\bar{M}^p+\mathbf{n}:\mathbf{E}:\mathbf{n}}\mathbf{E}:\mathbf{n}=\left(\mathbf{E}-\frac{\mathbf{E}:\mathbf{n}\otimes\mathbf{n}:\mathbf{E}}{\bar{M}^p+\mathbf{n}:\mathbf{E}:\mathbf{n}}\right):\mathbf{d}} \tag{7.34}$$

The loading criterion is given by

$$\left.\begin{array}{l}\mathbf{d}^p\neq\mathbf{O}\ \text{for}\ \dot{\Lambda}\ >0\\ \mathbf{d}^p=\mathbf{O}\ \text{for}\ \dot{\Lambda}\leq 0\end{array}\right\} \tag{7.35}$$

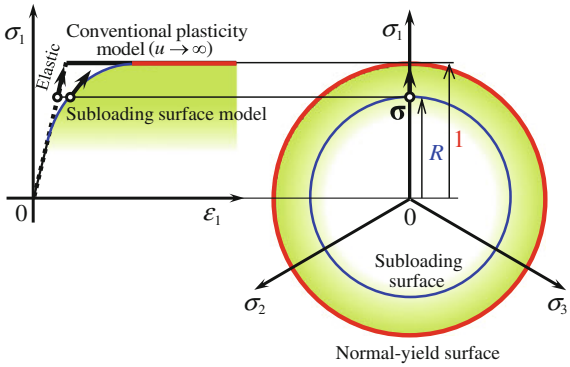

Fig. 7.10 Smooth stress–strain curve predicted by the subloading surface

or

$$\boxed{\begin{array}{l}\mathbf{d}^p \neq \mathbf{O}:\mathbf{n}:\mathbf{E}:\mathbf{d} > 0\\ \mathbf{d}^p = \mathbf{O}: \text{otherwise}\end{array}} \tag{7.36}$$

where the judgment whether or not the stress reaches the yield surface is not required since the plastic strain rate is induced continuously as the stress approaches the normal-yield surface.

There exists the risk that the subloading surface once contracts and then expands, so that a plastic strain rate is induced at the moment of stress reversal event in the neighborhood of the similarity-center of the normal-yield and the subloading surfaces even when $\mathbf{n} : \mathbf{E} : \mathbf{d} < 0$ holds. Therefore, the magnitude of input loading increment must be so small as to avoid the risk in the numerical calculation method.

The stress vs. strain curve by the subloading surface model is illustrated for the simplest case of the perfectly-plastic material in Fig. 7.10.

7.3 Salient Features of Subloading Surface Model

This model possesses the following distinguished abilities.

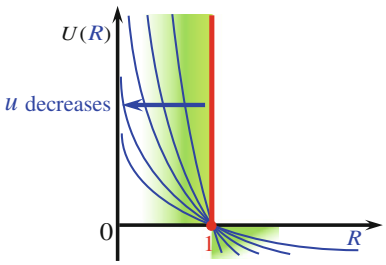

Fig. 7.11 Influence of u on function $U(R)$

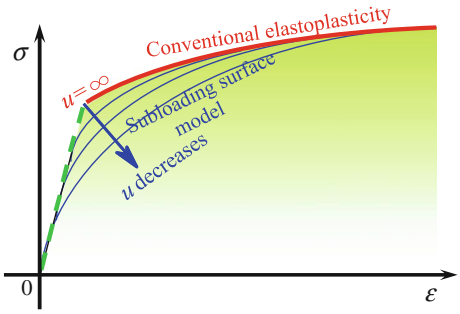

Fig. 7.12 Influence of u on stress–strain curve

(1) Smooth transition from elastic to plastic state is described, which is observed in real material behavior. Then, we don't need suffer from the determination of an offset value (plastic strain value in yield point). In contrast, the determination is required in all of the other elastoplastic models since they assume a surface enclosing a purely-elastic domain leading to the abrupt elastic-plastic transition, while the determination is accompanied with an arbitrariness. The influences of the material parameter u on the function $U(R)$ and the stress-strain curve are depicted in Figs. 7.11 and 7.12, respectively. The larger the material parameter u, the more rapidly the normal-yield ratio R increases causing the more rapid increase of stress, i.e. approaching the behavior of the conventional plasticity.
(2) Plastic strain rate can be described even for low stress level and for cyclic loading process under small stress amplitudes since a purely-elastic domain is not assumed.
(3) The yield-judgment whether or not the stress reaches the yield surface is unnecessary since the plastic strain rate develops continuously as the stress approaches the normal-yield surface. In contrast, the yield judgment is required

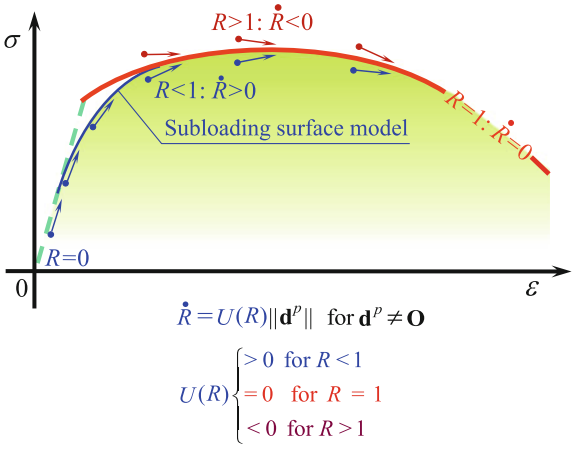

Fig. 7.13 Stress is automatically controlled to be attracted to the normal-yield surface in the subloading surface model

in all of the other elastoplastic models since they assume a surface enclosing a purely-elastic domain.

(4) The stress is automatically pulled back to the normal-yield surface when it goes over the surface in numerical calculation because of $\dot{R}<0$ for $R>1$ from Eq. (7.7) with Eq. $(7.11)_4$ as seen in Fig. 7.13. In contrast, the particular operation to pull back the stress is required in all of the other models because they assume a surface enclosing a purely-elastic domain.

For the normal-yield state $R=1$ ($U=0$), the plastic strain rate in Eq. (7.29) with Eq. (7.30) is reduced to Eq. (6.43) with Eq. (6.41) for the conventional plasticity, i.e.

$$\mathbf{d}^p=\frac{\mathbf{n}:\mathring{\boldsymbol{\sigma}}}{\frac{F'}{F}f_{Hn}(\boldsymbol{\sigma},H;\mathbf{n})\mathbf{n}:\boldsymbol{\sigma}}\mathbf{n}\left(=\frac{\dfrac{\partial f(\boldsymbol{\sigma})}{\partial\boldsymbol{\sigma}}:\mathring{\boldsymbol{\sigma}}}{F'f_{Hn}\left(\boldsymbol{\sigma},H;\dfrac{\partial f(\boldsymbol{\sigma})}{\partial\boldsymbol{\sigma}}\right)}\frac{\partial f(\boldsymbol{\sigma})}{\partial\boldsymbol{\sigma}}\right)$$

For $u\to\infty$ leading to the sudden decrease of the function U from $U\to\infty$ for $R<1$ to $U=0$ for $R=1$ in Eq. (7.11), the plastic modulus $\bar{M}^p$ in Eq. (7.30) drops suddenly from the infinite value to the value M^p in Eq. (6.41) so that the present model behavior is reduced to the conventional elastoplasticity model behavior by choosing a large value of the material parameter u, thereby exhibiting an sudden transition from the elastic to plastic state. On the other hand, as u becomes smaller, a gentler transition from the elastic to plastic state is described. Therefore, u plays the role to alleviate the sudden transition from the elastic to plastic state.

It follows from Eq. (6.43) and Eq. (7.29) in the plastic loading process, fulfilling $\dot{\lambda}\geq 0$ or $\dot{\bar{\lambda}}\geq 0$, that

$$\left.\begin{aligned}&M^p>0\to\mathbf{n}:\mathring{\boldsymbol{\sigma}}>0,\ \dot{F}>0:\text{normal hardening}\\&M^p=0\to\mathbf{n}:\mathring{\boldsymbol{\sigma}}=0,\ \dot{F}=0:\text{normal nonhardening}\\&M^p<0\to\mathbf{n}:\mathring{\boldsymbol{\sigma}}<0,\ \dot{F}<0:\text{normal softening}\end{aligned}\right\}\tag{7.37}$$

for the conventional model and

$$\left.\begin{aligned}&\bar{M}^p>0\to\mathbf{n}:\mathring{\boldsymbol{\sigma}}>0:\text{subloading hardening}\\&\bar{M}^p=0\to\mathbf{n}:\mathring{\boldsymbol{\sigma}}=0:\text{subloading nonhardening}\\&\bar{M}^p<0\to\mathbf{n}:\mathring{\boldsymbol{\sigma}}<0:\text{subloading softening}\end{aligned}\right\}\tag{7.38}$$

for the subloading surface model. Here, it should be noted that the signs of M^p or $\bar{M}^p$ and $\mathbf{n}:\mathring{\boldsymbol{\sigma}}$ coincide with each other in both models but they do not necessarily coincide with the sign of $\dot{F}$ in the subloading surface model.

The distinguished advantages of the subloading surface model in the descriptions of irreversible mechanical phenomena can be obtained by the simple

modification of existing computer program for the conventional elastoplasticity model to add only one material parameter u for the evolution rule of the normal-yield ratio without any expense.

7.4 Numerical Performance of Subloading Surface Model

The stress controlling function of the subloading surface model is described in Sect. 7.3. This fact will be shown below by the numerical calculation for the response of the uniaxial loading behavior, adopting the simplest subloading surface model for the isotropic Mises material with the evolution rule of the normal-yield ratio in Eq. (7.9) with Eq. (7.12). The response of the conventional elastoplastic constitutive model is also shown for the comparison.

The relations of the axial stress σ_a and the normal-yield ratio R versus the axial strain ε_a are depicted in Fig. 7.14. The responses adopting the linear isotropic hardening $F = F_0 + h_c\varepsilon^{ep}$ (h_c: material constant) are depicted in Fig. 7.14a and those for the nonlinear isotropic hardening in Eq. (6.56) are shown in Fig. 7.14b. The two levels of axial strain increment $d\varepsilon_a = 0.0006$ and 0.0055 are input in the numerical calculations. Here, any special stress controlling algorithm to pull it back to the yield surface is not introduced. The material parameters are chosen as follows:

Material constants:

$$\begin{aligned}&\text{Young's modulus: } E = 100000\text{MPa},\\ &\text{Hardening}\begin{cases}\text{Linear isotropic: } h_c = 7000\text{MPa}\\ \text{Nonlinar isotropic: } h_1 = 0.8,\ h_2 = 50,\end{cases}\\ &\text{Evolution of normal - yield ratio : } u = 200.\end{aligned}$$

Initial values:

$$\begin{aligned}&\text{Hardening function: } F_0 = 500\text{MPa},\\ &\text{Stress : } \boldsymbol{\sigma}_0 = \mathbf{O}\text{MPa}\end{aligned}$$

The nonsmooth curves bent at the yield stress are expressed by the conventional model. Moreover, the stress deviates from the exact curve of conventional elastoplasticity. The deviation becomes large with the increases in the nonlinearity of hardening and in the increase of input strain increment. On the other hand, the stress is automatically attracted to the normal-yield surface in the subloading surface model even for the quite large strain increment $d\varepsilon_a = 0.0055\,(0.55\%)$. The zigzag lines tracing the exact curve are calculated such that the stress rises up when the it lies below the normal-yield surface but it drops down immediately if it goes

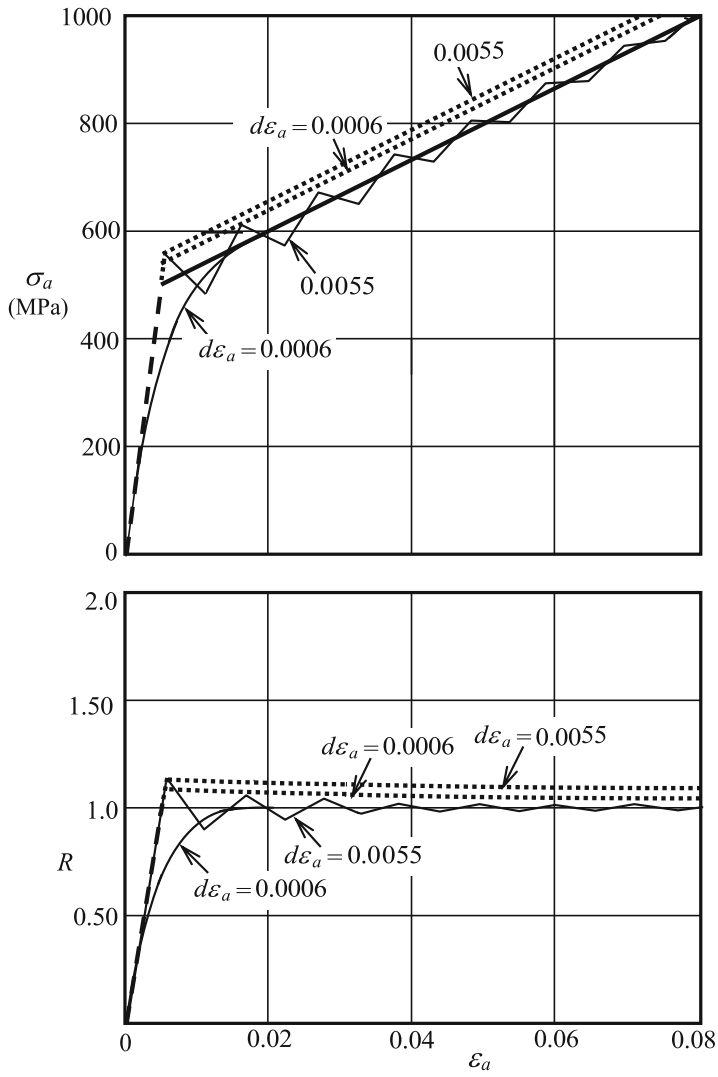

(a) Linear isotropic hardening

Exact curve of conventional elastoplasticity
Calculated by the conventional elastoplastic model
Calculated by the subloading surface model

Fig. 7.14 Numerical accuracies of the conventional elastoplastic and the subloading surface model: Uniaxial loading behavior of Mises material with isotropic hardening. **a** Linear isotropic hardening **b** nonlinear isotropic hardening (continued)

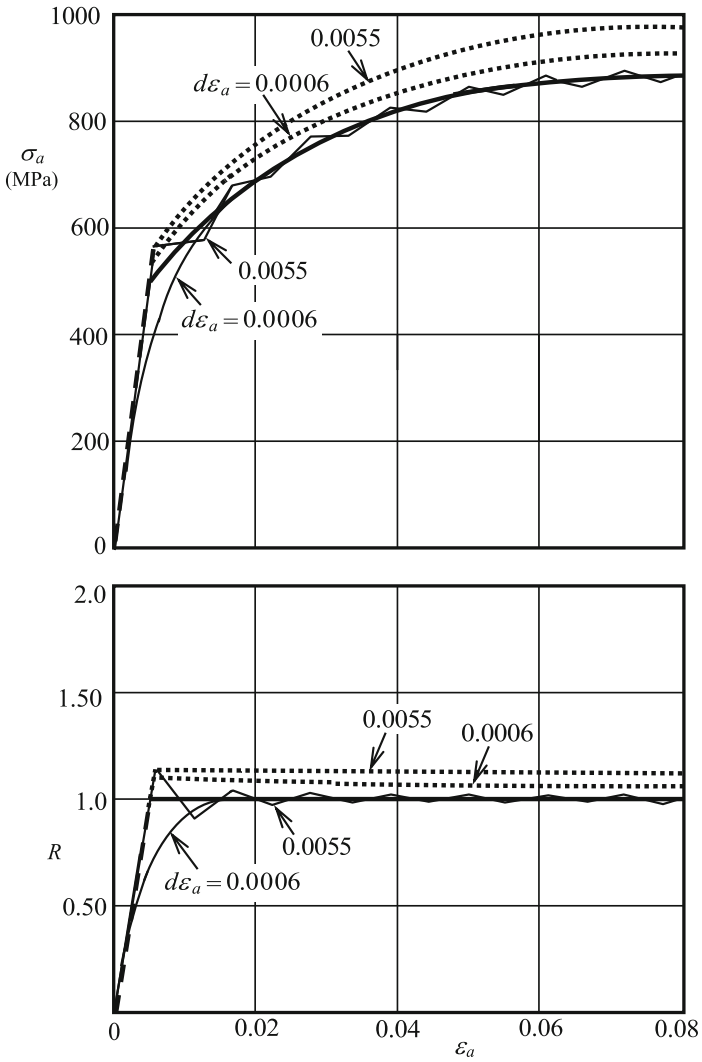

(b) Nonlinear isotropic hardening

Fig. 7.14 (continued)

over the normal-yield surface, obeying the evolution rule of normal-yield ratio in Eq. (7.9) with Eq. (7.12), i.e. $\dot{R} > 0$ for $R < 1$ and $\dot{R} < 0$ for $R > 1$. The plastic modulus $\bar{M}^p$ lowers than that in the conventional one and further it can be negative at the over normal-yield state $R > 1$ leading to $U < 0$, while $\mathbf{n} : \mathring{\boldsymbol{\sigma}} < 0$ (subloading

softening defined in Eq. (7.38)) holds for $\bar{M}^p < 0$ because of $\dot{\lambda} > 0$ as known from Eqs. (7.29–7.31). The amplitude of zigzag decreases gradually in the monotonic loading process, while, needless to say, the amplitude is smaller for a smaller input increment of strain. Eventually, the subloading surface model posseses the distinguished high ability for numerical calculation as verified also quantitatively in these concrete examples, which has not been attained in any other elastoplastic constitutive equations including the multi, the two, the infinite, superposed kinematic hardening and the bounding surface models assuming a purely-elastic domain as will be described in Chap. 8.

7.5 On Bounding Surface and Bounding Surface Model

The terms *bounding surface* and *bounding surface model* are widely used for models falling within the framework of unconventional plasticity describing the plastic strain rate induced by the rate of stress inside the yield surface. They were named by Y. F. Dafalias, who also coined the terms *plastic spin* (Dafalias 1985a) and *hypoplasticity* (Dafalias 1986). The only concrete model proposed by Dafalias as the bounding surface model is the two-surface model (Dafalias and Popov 1975), in which a small subyield surface is assumed inside the yield surface. The small subyield surface encloses the purely elastic domain and translates maintaining the size which maintains constant ratio to the size of the bounding surface (Dafalias and Popov 1977). On the other hand, the basic structure of the *bounding surface model with a radial mapping* used later by Dafalias and Herrmann (1980) falls within the framework of the subloading surface model, as has been recognized by Dafalias himself in his statement "*It appears that the first time a radial mapping formulation was proposed, it was in reference to granular materials by Hashiguchi and Ueno (1977)*" which is the original sentence in Dafalias (1986, p. 980).

However, note the following facts.

(1) The bounding surface is no more than the yield surface that has been assumed historically in the field of plasticity. The term yield surface has a clear physical meaning that the plastic deformation begins when stress reaches it; it also has the geometrical meaning that the stress cannot go out from it in the quasi-static deformation process. In contrast, the phrase bounding surface has only a geometrical meaning but has no physical meaning.

(2) The yield surface always exists. However, the stress goes over the yield surface in the deformation process at a high rate as represented by the *overstress model* describing a viscoplastic deformation. Therefore, no surface exists which bounds the stress except for the quasi-static deformation process. Consequently, the phrase "bounding surface" has no generality.

(3) The term bounding surface model induces the confusion as if all unconventional plasticity models inheriting the yield surface belong to the bounding surface model. Krieg (1975) uses the term *limit surface* in his two surface

model, Mroz (1967) uses *outmost surface* in his *multi surface model*, and Hashiguchi (1989) uses *normal-yield surface* in his *subloading surface model* instead of yield surface. However, they use these words only in a limited sense for naming elements in their models: they never use these words as names of their proposed models such as the *limit surface model*, the *outmost surface model*, or the *normal-yield surface model*. The term bounding surface should be used only for the two surface model of Dafalias and Popov (1975) in order to avoid the confusion.

Furthermore, Dafalias uses the phrase *bounding surface model with a radial mapping* (Dafalias and Herrmann 1980). Nevertheless, it possesses physical and mathematical structure which differs from the two-surface model but it is based on the identical basic structure to the subloading surface model proposed in 1977 three years earlier than 1980 when Dafalias began to write the articles on the bounding surface model with a radial mapping. Furthermore, it includes various the immaturity and the impertinence in the explicit formulations as described below.

In the bounding surface model with a radial mapping, the following ratio is adopted as the measure to describe the degree of approaching the yield (bounding) surface.

$$b \equiv ||\boldsymbol{\sigma}_y||/||\boldsymbol{\sigma}|| \, (1 \leq b \leq \infty) \tag{7.39}$$

which is the ratio of the magnitude of conjugate stress $\boldsymbol{\sigma}_y$ on the yield surface to the magnitude of current stress $\boldsymbol{\sigma}$. Then, the plastic modulus M^p in the plastic strain rate of the conventional plasticity, i.e. Eq. (6.41) is modified merely by the interpolation method without incorporation of the consistency condition as

$$M^p \to M^p + \hat{H}\langle\frac{b-1}{b_e-b}\rangle \left(= \begin{cases} \to \infty & \text{for } b \geq b_e \\ M^p & \text{for } b = 1 \end{cases} \right) \tag{7.40}$$

where $\hat{H}$ is the function of stress and internal variables and b_e is the value of the variable b at the elastic limit.

Here, note the following facts.

(i) The variable $b(\infty \geq b \geq 1)$ is merely the inverse of normal-yield ratio $R(0 \leq R \leq 1)$ in the subloading surface model, whilst $b \to \infty$ and $b = 1$ correspond to $R = 0$ and $R = 1$, respectively.

(ii) The plastic modulus M^p in the bounding surface model with a radial mapping is given by the interpolation method between the stress in an elastic limit and the stress on the yield (bounding) surface, where no consistency condition is introduced as can be confirmed from the statement "*No consistency condition* $\dot{f} = 0$ *is required for stress points inside* $F = 0$*, since now* $f = 0$ *is always defined at any* σ_{ij}." (Dafalias 1986, p. 978), whereas the consistency condition for the subloading surface is introduced into the subloading surface model. Various equations other than Eq. (7.40) can be

assumed for the plastic modulus if an easy-going interpolation method is adopted. In fact, Eq. (7.40) differs substantially from the plastic modulus of Eq. (7.30) in the subloading surface model which is derived rigorously from the consistency condition formulated based on the assumption that the normal-yield ratio approaches unity in the plastic loading process.

(iii) Therefore, it is not guaranteed that the stress approaches the yield surface in the plastic loading process. On the other hand, the subloading surface model possesses a stress controlling function to attract the stress to the yield surface in the plastic loading process even if the stress goes out from the yield surface in the numerical calculation by the finite strain or stress increments.

(iv) A formulation for describing cyclic loading behavior has not been given for the bounding surface model with a radial mapping. On the other hand, it was attained in the subloading surface model as the *extended subloading surface model* (Hashiguchi 1989) by making the similarity-center of the normal-yield and the subloading surfaces move with the plastic strain rate as will be described in detail in the next chapter.

Eventually, it can be concluded for the bounding surface model with radial mapping as follows:

(I) The bounding surface is substantially the synonym of the yield surface although it does not express any physical meaning. Therefore, the term: bounding surface model would cause confusion as if all models adopting the yield surface belong to this model, while in fact it is insisted by Dafalias that *the model with "stress reversal surfaces" (infinite surface model of* Mroz et al. 1981) *proposed for soils can be classified as a radial mapping model* (Dafalias 1986, p. 981) in addition to the impertinent assessment on the subloading surface model. It is desirable to make effort for concrete formulation of pertinent model rather than only coining new terms. Eventually, the term bounding surface should be used only for the two surface model formulated by Dafalias himself.

(II) The bounding surface model with radial mapping falls within the framework of the subloading surface model but it is not formulated rationally, whereas the rigorous formulations including the description of cyclic loading behavior have been given by the subloading surface model.

Eventually, the ones using the bounding surface with radial mapping should abandon its use and instead they should notice the subloading surface model for rigorous deformation analyses and sound development of plasticity.

7.6 Incorporation of Kinematic Hardening

The subloading surface based on the yield surface in Eq. (6.85) with the kinematic hardening is described as

$$f(\hat{\boldsymbol{\sigma}}) = RF(H) \tag{7.41}$$

The material-time derivative of Eq. (7.41) leads to

$$\frac{\partial f(\hat{\boldsymbol{\sigma}})}{\partial \hat{\boldsymbol{\sigma}}} : \mathring{\boldsymbol{\sigma}} - \frac{\partial f(\hat{\boldsymbol{\sigma}})}{\partial \hat{\boldsymbol{\sigma}}} : \mathring{\boldsymbol{\alpha}} - RF' \dot{H} - \dot{R} F = 0 \tag{7.42}$$

Substituting the associated flow rule

$$\mathbf{d}^p = \dot{\bar{\lambda}} \hat{\mathbf{n}} \ (\dot{\bar{\lambda}} = ||\mathbf{d}^p|| \geq 0) \tag{7.43}$$

Eq. (7.42) is rewritten substituting Eq. (6.88) as

$$\frac{\partial f(\hat{\boldsymbol{\sigma}})}{\partial \hat{\boldsymbol{\sigma}}} : \mathring{\boldsymbol{\sigma}} - \frac{\partial f(\hat{\boldsymbol{\sigma}})}{\partial \hat{\boldsymbol{\sigma}}} : \dot{\bar{\lambda}} \mathbf{f}_{kn}(\boldsymbol{\sigma}, \boldsymbol{\alpha}, F; \hat{\mathbf{n}}') - RF' \dot{\bar{\lambda}} f_{Hn}(\boldsymbol{\sigma}, H; \hat{\mathbf{n}}) - U \dot{\bar{\lambda}} F = 0 \tag{7.44}$$

Noting

$$\left.\begin{aligned} &\frac{\partial f(\hat{\boldsymbol{\sigma}})}{\partial \hat{\boldsymbol{\sigma}}} : \hat{\boldsymbol{\sigma}} = f(\hat{\boldsymbol{\sigma}}) = RF \\ &\frac{\partial f(\hat{\boldsymbol{\sigma}})}{\partial \hat{\boldsymbol{\sigma}}} = ||\frac{\partial f(\hat{\boldsymbol{\sigma}})}{\partial \hat{\boldsymbol{\sigma}}}|| \hat{\mathbf{n}} \\ &1/||\frac{\partial f(\hat{\boldsymbol{\sigma}})}{\partial \hat{\boldsymbol{\sigma}}}|| = \frac{\dfrac{\partial f(\hat{\boldsymbol{\sigma}})}{\partial \hat{\boldsymbol{\sigma}}} : \hat{\boldsymbol{\sigma}}}{f(\hat{\boldsymbol{\sigma}})} / ||\frac{\partial f(\hat{\boldsymbol{\sigma}})}{\partial \hat{\boldsymbol{\sigma}}}|| = \frac{\hat{\mathbf{n}} : \hat{\boldsymbol{\sigma}}}{RF} \end{aligned}\right\} \tag{7.45}$$

Equation (7.44) is rewritten as

$$\hat{\mathbf{n}} : \mathring{\boldsymbol{\sigma}} - \hat{\mathbf{n}} : \dot{\bar{\lambda}} \mathbf{f}_{kn}(\boldsymbol{\sigma}, \boldsymbol{\alpha}, F; \hat{\mathbf{n}}') - \hat{\mathbf{n}} : \hat{\boldsymbol{\sigma}} \left(\frac{F'}{F} \dot{\bar{\lambda}} f_{Hn}(\boldsymbol{\sigma}, H; \hat{\mathbf{n}}) + \frac{U}{R} \dot{\bar{\lambda}} \right) = 0 \tag{7.46}$$

from which one has

$$\dot{\bar{\lambda}} = \frac{\hat{\mathbf{n}} : \mathring{\boldsymbol{\sigma}}}{\bar{M}^p}, \ \mathbf{d}^p = \frac{\hat{\mathbf{n}} : \mathring{\boldsymbol{\sigma}}}{\bar{M}^p} \hat{\mathbf{n}} \tag{7.47}$$

where

$$\bar{M}^p \equiv \hat{\mathbf{n}} : \left[\left(\frac{F'}{F} f_{Hn}(\boldsymbol{\sigma}, H; \hat{\mathbf{n}}) + \frac{U}{R} \right) \hat{\boldsymbol{\sigma}} + \mathbf{f}_{kn}(\boldsymbol{\sigma}, \boldsymbol{\alpha}, F; \hat{\mathbf{n}}') \right] \tag{7.48}$$

The loading criterion is given by

$$\left. \begin{array}{l} \mathbf{d}^p \neq \mathbf{O} : \hat{\mathbf{n}} : \mathbf{E} : \mathbf{d} > 0 \\ \mathbf{d}^p = \mathbf{O} : \text{ otherwise} \end{array} \right\} \tag{7.49}$$

7.7 Incorporation of Tangential-Inelastic Strain Rate

As presented in Eqs. (6.43) and (6.95), the inelastic strain rate in the traditional constitutive equation has the following limitations.

(i) The inelastic strain rate depends solely on the stress rate component normal to the yield surface, called the *normal stress rate*, but is independent of the component tangential to the yield surface, called the *tangential stress rate*, since it is derived merely based on the consistency condition.
(ii) The direction of inelastic strain rate is determined solely by the current state of stress and internal variables but it is independent of the stress rate.
(iii) The principal directions of inelastic strain rate tensor coincide with those of stress tensor, exhibiting the so-called *coaxiality*, in the case of isotropy in which the direction of plastic strain rate depends only on the direction of stress by the fact described in Sect. 1.12.

On the other hand, it has been verified by experiments that an inelastic strain rate induced by the deviatoric part of the tangential stress rate, called the *deviatoric tangential stress rate*, influences considerably on a deformation in the non-proportional loading process deviating from the proportional loading path normal to the yield surface, which is called the *tangential inelastic strain rate*. Here, the spherical part of the tangential stress rate does not induce an inelastic strain rate, as Rudnicki and Rice (1975) verified based on the fissure model. In addition, the tangential inelastic strain rate is induced considerably in the plastic instability phenomena with the strain localization induced by the generation of the shear band and it influences on the macroscopic deformation and strength characteristics. To remedy these insufficiencies of the traditional plastic constitutive equation, various models have been proposed to date as follows:

(1) *Intersection of plural yield surfaces*: Various models assuming the intersection of plural yield surfaces have been proposed (Batdorf and Budiansky 1949; Koiter 1953; Bland 1957; Mandel 1965; Hill 1966; Sewell 1973, 1974). The Koiter's (1953) model was adopted by Sewell (1973, 1974), but it is indicated that the applicability of the model is limited to the inception of uniaxial loading. Models in this category cannot describe the latent hardening pertinently and are

not readily applicable to general loading processes (cf. Christoffersen and Hutchinson (1979)).

(2) *Corner theory*: The singularity of outward-normal of the yield surface is introduced by assuming the conical corner or vertex at the stress point on the yield surface. Therefore, the direction of plastic strain rate can take a wide range surrounded by the outward-normal of the yield surface (Christoffersen and Hutchinson 1979; Ito 1979; Gotoh 1985; Goya and Ito 1991; Petryk and Thermann 1997). There exist the two kinds of models: One kind is based on the assumption of an imaginary infinitesimal vertex and the other subsumes a finite projecting cone. The evolution rule of the cone cannot be formulated and the reloading from the cone surface after partial unloading cannot be described pertinently in the latter models. It was described by Hecker (1972) and Ikegami (1979) that the yield surface projects towards the loading direction generally but the formation of the so-called vertex is doubtful.

(3) *Hypoplasticity*: This term was first used by Dafalias (1986) in the analogy to the term hypoelasticity introduced by Truesdell (1955) described in Sect. 5.4. Models in this category are classified into the two kind of models in which the direction of plastic strain rate depends on the direction of the stress rate $\mathring{\boldsymbol{\sigma}}/||\mathring{\boldsymbol{\sigma}}||$ (Mroz 1966; Dafalias and Popov 1977; Hughes and Shakib 1986; Wang et al. 1990; Hashiguchi 1993a) and the models in which the direction of the plastic strain rate depends on the direction of strain rate $\mathbf{d}/||\mathbf{d}||$ (Hill 1959; Simo 1987; Hashiguchi 1997). The singularity in the field of direction of plastic strain rate is introduced in the algebraic ways into these models, although it is done geometrically in the models described in (1) and (2). However, the magnitude of the plastic strain rate is derived from the consistency condition. Therefore, the plastic strain rate diminishes when the stress rate is directed tangentially to the yield surface, as in the traditional constitutive equations without the vertex.

The constitutive equations described in (1)–(3) possess the following problems.

(i) A formulation of pertinent model which fulfills the consistency condition and is applicable to the general loading process is difficult.

(ii) The stress rate vs. strain rate relation becomes nonlinear. Therefore, the inverse expression cannot be derived, which renders deformation analysis as difficult.

Differently from the above-mentioned models, the following linear relation between the stress rate vs. strain rate with the tangential-inelastic strain rate, called the J_2- *deformation theory*, has been formulated by Budiansky (1959) and later Rudnicki and Rice (1975) by extending Eq. (6.59) with the isotropic Mises yield condition as follows:

$$\mathbf{d}=\mathbf{E}^{-1}:\mathring{\boldsymbol{\sigma}}+\frac{3}{2}\frac{1}{F'}\frac{\dot{\sigma}^{eq}}{\sigma^{eq}}\boldsymbol{\sigma}'+\phi(\sigma^{eq})\left[\mathring{\boldsymbol{\sigma}}'-\left(\frac{\boldsymbol{\sigma}'}{||\boldsymbol{\sigma}'||}:\mathring{\boldsymbol{\sigma}}'\right)\frac{\boldsymbol{\sigma}'}{||\boldsymbol{\sigma}'||}\right] \tag{7.50}$$

which can be rewritten as

$$\begin{aligned}\mathbf{d} &= \mathbf{E}^{-1} : \mathring{\boldsymbol{\sigma}} \ + \ \frac{3}{2}\frac{1}{F'}\frac{\dot{\sigma}^{eq}}{\sigma^{eq}}\boldsymbol{\sigma}' \ + \ \phi(\sigma^{eq})\left(\mathring{\boldsymbol{\sigma}}' - \sqrt{2/3}\dot{\sigma}^{eq}\frac{\boldsymbol{\sigma}'}{\sqrt{2/3}\sigma^{eq}}\right) \\ &= \mathbf{E}^{-1} : \mathring{\boldsymbol{\sigma}} + \left(\frac{3}{2}\frac{1}{F'} - \phi(\sigma^{eq})\right)\frac{\dot{\sigma}^{eq}}{\sigma^{eq}}\boldsymbol{\sigma}' \ + \ \phi(\sigma^{eq})\mathring{\boldsymbol{\sigma}}'\end{aligned} \tag{7.51}$$

where the rate-linearity is retained.

On the other hand, *Hencky's deformation theory* (Hencky 1924) is described as

$$\boldsymbol{\varepsilon} = \mathbf{E}^{-1} : \sigma \ + \ \phi(\sigma^{eq})\boldsymbol{\sigma}' \tag{7.52}$$

The corotational time-derivative of Eq. (7.52) leads to

$$\mathring{\boldsymbol{\varepsilon}} = \mathbf{E}^{-1} : \mathring{\boldsymbol{\sigma}} \ + \ \phi'(\sigma^{eq})\dot{\sigma}^{eq}\boldsymbol{\sigma}' \ + \ \phi(\sigma^{eq})\mathring{\boldsymbol{\sigma}}' \tag{7.53}$$

Comparing Eq. (7.51) with Eq. (7.53), choosing $F(\sigma^{eq})$ so as to fulfill

$$F'(\varepsilon^{eqp}(\sigma^{eq})) = \frac{3}{2}\frac{1}{\phi(\sigma^{eq}) \ + \ \phi'(\sigma^{eq})\sigma^{eq}} \tag{7.54}$$

and regarding $\mathbf{d}$ as $\mathring{\boldsymbol{\varepsilon}}$, it is known that the J_2- deformation theory coincides with Hencky's deformation theory (7.52). However, it possesses crucial limitations as described in below.

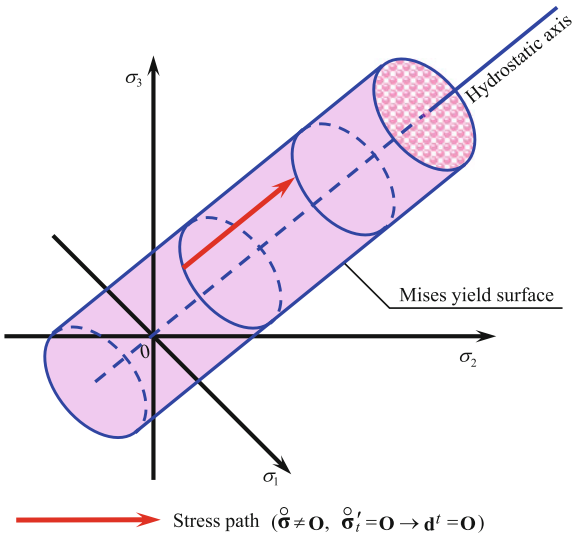

Fig. 7.15 Example showing the fact that tangential-inelastic strain rate is not induced by spherical stress rate since inelastic volumetric change is not induced in metals

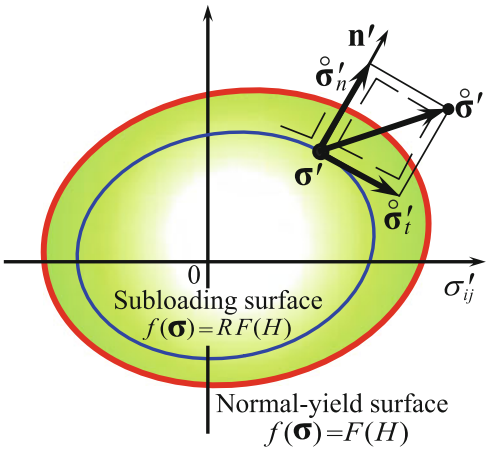

Fig. 7.16 Normal and tangential stress rates for subloading surface model in deviatoric stress plane

In what follows, let the tangential inelastic strain rate be incorporated into the above-mentioned subloading surface model in the following (Hashiguchi 1998, 2005; Hashiguchi and Tsutsumi 2003; Hashiguchi and Protasov 2004; Khojastepour and Hashiguchi 2004a, b; Khojastehpour et al. 2006).

Inelastic strain rate is induced even by the deviatoric stress rate component tangential to the loading surface in real material behavior, while it would not be induced by spherical stress rate as would be inferred from the example for the fact that inelastic volumetric change would not be induced in metals (see Fig. 7.15). However, this fact has been ignored in the traditional plasticity described in the preceding sections in which the inelastic strain rate is given only by the plastic strain rate derived from the consistency condition of the subloading surface so that it is depends only on the stress rate component normal to the subloading surface.

In order to describe the inelastic strain rate induced by the deviatoric stress rate component tangential to the subloading surface, assume that the strain rate is additively composed of the elastic strain rate, the plastic strain rate and the *tangential-inelastic strain rate* $\mathbf{d}^t$ as follows (Hashiguchi, 1998, 2013b, 2016):

$$\mathbf{d} = \mathbf{d}^e + \mathbf{d}^p + \mathbf{d}^t \tag{7.55}$$

Further, assume that the tangential-inelastic strain rate $\mathbf{d}^t$ is induced by the tangential component of the stress rate $\overset{\circ}{\boldsymbol{\sigma}}$ to the subloading surface in the deviatoric stress space, which is denoted by $\overset{\circ}{\boldsymbol{\sigma}}{}'_t$ (Fig. 7.16) defined by

$$\left.\begin{aligned}\mathring{\boldsymbol{\sigma}}_t^{'} &\equiv \mathfrak{T}_t' : \mathring{\boldsymbol{\sigma}} = \mathring{\boldsymbol{\sigma}}^{'} - \mathring{\boldsymbol{\sigma}}_n^{'} (\mathbf{n} : \mathring{\boldsymbol{\sigma}}_t^{'} = \mathfrak{n}' : \mathring{\boldsymbol{\sigma}}_t^{'} = 0) \\ \mathring{\boldsymbol{\sigma}}_n^{'} &\equiv (\mathfrak{n}' : \mathring{\boldsymbol{\sigma}})\mathfrak{n}' = (\mathfrak{n}' \otimes \mathfrak{n}') : \mathring{\boldsymbol{\sigma}}\end{aligned}\right\} \tag{7.56}$$

$$\mathfrak{n}' \equiv \frac{\mathfrak{n}'}{||\mathfrak{n}'||} = \left(\frac{\partial f(\boldsymbol{\sigma})}{\partial \boldsymbol{\sigma}}\right)' \Big/ \left|\left|\left(\frac{\partial f(\boldsymbol{\sigma})}{\partial \boldsymbol{\sigma}}\right)'\right|\right| \left(\neq \mathfrak{n}' = \left(\frac{\partial f(\boldsymbol{\sigma})}{\partial \boldsymbol{\sigma}}\right)' \Big/ \left|\left| \frac{\partial f(\boldsymbol{\sigma})}{\partial \boldsymbol{\sigma}} \right|\right| \right) (||\mathfrak{n}'|| = 1) \tag{7.57}$$

$$\mathfrak{T}_t' \equiv \mathcal{I}' - \mathfrak{n}' \otimes \mathfrak{n}', \ \mathfrak{T}_{ijkl}' \equiv \mathcal{I}_{ijkl}' - \mathfrak{n}_{ij}' \mathfrak{n}_{kl}' \tag{7.58}$$

fulfilling

$$\mathfrak{n}_t' \equiv \mathfrak{T}_t' : \mathfrak{n} = \mathfrak{n}' - (\mathfrak{n}' : \mathfrak{n})\mathfrak{n}' = \mathbf{O} \tag{7.59}$$

The fourth-order tensor $\mathcal{I}'$ is the *deviatoric projection tensor* in Eq. (1.146). The fourth-order tensor $\mathfrak{T}_t'$ is the *deviatoric-tangential projection tensor* which transforms an arbitrary second-order tensor to the tangential part to the subloading surface in the deviatoric stress space and the second-order tensor subjected to this projection is designated by $(\,)_t'$, i.e. $\mathfrak{t}_t' \equiv \mathfrak{T}_t' : \mathfrak{t}$ leading further to $\mathfrak{T}_t' : \mathfrak{t}_t' = \mathfrak{t}_t'$. Then, $\mathring{\boldsymbol{\sigma}}_t'$ is the deviatoric-tangential projection tensor of the stress rate $\mathring{\boldsymbol{\sigma}}$, which is called the *deviatoric-tangential stress rate*.

Now, assume that the tangential-inelastic strain rate $\mathbf{d}^t$ is related linearly to the tangential-deviatoric stress rate $\mathring{\boldsymbol{\sigma}}_t'$ by the extended hypoelastic relation (Truesdell 1955) in the normal-yield state ($R = 1$) as follows:

$$\mathbf{d}^t = \mathbf{E}^{-1} : \mathring{\boldsymbol{\sigma}}_t' \tag{7.60}$$

where $\mathbf{E}$ is the fourth-order tensor which is a function of stress and internal variables in general. Let Eq. (7.60) be extended for the sub-yield state as follows:

$$\mathbf{d}^t = T(R)\mathbf{E}^{-1} : \mathring{\boldsymbol{\sigma}}_t' \tag{7.61}$$

In this equation $T(R)$ is the monotonically-increasing function of R given by

$$\boxed{T(R) = \tilde{c}R^{\tilde{n}}} \tag{7.62}$$

or

$$T(R) = \tilde{c}\left\langle \frac{R - \tilde{R}_e}{1 - \tilde{R}_e} \right\rangle^{\tilde{n}} \left(\begin{cases} = 0 \text{ for } R \le \tilde{R}_e \\ > 0 \text{ for } \tilde{R}_e < R < 1 \\ = \tilde{c} \text{ for } R = 1 \end{cases} \right) \tag{7.63}$$

where $\tilde{c}$, $\tilde{n}(\geq 1)$ and $\tilde{R}_e$ (<1) are the material constants. The tangential-inelastic strain rate is induced increasingly as the stress approaches the normal-yield surface, always fulfilling the continuity and the smoothness conditions (Hashiguchi 1993a,b, 1997, 2000). On the other hand, if the tangential-inelastic strain rate is incorporated into the plasticity model assuming the yield surface enclosing a purely-elastic domain, both of the continuity and the smoothness conditions are violated, since the tangential-inelastic strain rate is induced suddenly at the moment when the stress reaches the yield surface.

Adding the tangential-inelastic strain rate in Eq. (7.62) to Eq. (7.32), the strain rate is given by

$$\begin{aligned}\mathbf{d} &= \mathbf{E}^{-1}\mathbf{:}\mathring{\boldsymbol{\sigma}} + \frac{\mathbf{n}\mathbf{:}\mathring{\boldsymbol{\sigma}}}{\bar{M}^p}\mathbf{n} + T(R)\mathbf{E}^{-1}\mathbf{:}\mathring{\boldsymbol{\sigma}}'_t \\ &= \left(\mathbf{E}^{-1} + \frac{\mathbf{n}\otimes\mathbf{n}}{\bar{M}^p} + T(R)\mathbf{E}^{-1}\mathbf{:}\mathfrak{T}'_t\right)\mathbf{:}\mathring{\boldsymbol{\sigma}}\end{aligned} \tag{7.64}$$

In what follows, we assume the elastic modulus tensor $\mathbf{E}$ fulfilling

$$\mathfrak{T}'_t\mathbf{:E:n} = \mathbf{O} \tag{7.65}$$

which holds in the Hooke's law in (Eq. 5.35) for example. Taking account of Eq. (7.65), it follows from Eq. (7.64) that

$$\mathfrak{T}'_t\mathbf{:E:d} = (1+T(R))\mathring{\boldsymbol{\sigma}}'_t \tag{7.66}$$

leading to

$$\mathring{\boldsymbol{\sigma}}'_t = \frac{1}{1+T(R)}\mathfrak{T}'_t\mathbf{:E:d} \tag{7.67}$$

Substituting Eq. (7.67) into Eq. (7.61), one obtains

$$\mathbf{d}^t - \frac{T(R)}{1+T(R)}\mathbf{E}^{-1}\mathfrak{T}'_t\mathbf{:E:}\,\mathbf{d} \tag{7.68}$$

The expression in Eq. (7.33) itself for the plastic multiplier in terms of strain rate is obtained from Eq. (7.64), noting Eq. (7.59). Then, the stress rate is given by substituting Eq. (7.55) with Eq. (7.34) and Eq. (7.68) into the relation $\mathring{\boldsymbol{\sigma}} = \mathbf{E}\mathbf{:}\mathbf{d}^e$ in Eq. (6.29) as follows:

$$\begin{aligned}\mathring{\boldsymbol{\sigma}} &= \mathbf{E}\mathbf{:}(\mathbf{d}-\mathbf{d}^p-\mathbf{d}^t) = \mathbf{E}\mathbf{:}\mathbf{d} - \frac{\mathbf{n}\mathbf{:}\mathbf{E}\mathbf{:}\mathbf{d}}{\bar{M}^p+\mathbf{n}\mathbf{:}\mathbf{E}\mathbf{:}\mathbf{n}}\mathbf{E}\mathbf{:}\mathbf{n} - \frac{T(R)}{1+T(R)}\mathfrak{T}'_t\mathbf{:E:d} \\ &= \left(\mathbf{E} - \frac{\mathbf{E}\mathbf{:}\mathbf{n}\otimes\mathbf{n}\mathbf{:}\mathbf{E}}{\bar{M}^p+\mathbf{n}\mathbf{:}\mathbf{E}\mathbf{:}\mathbf{n}} - \frac{T(R)}{1+T(R)}\mathfrak{T}'_t\mathbf{:E}\right)\mathbf{:}\mathbf{d}\end{aligned} \tag{7.69}$$

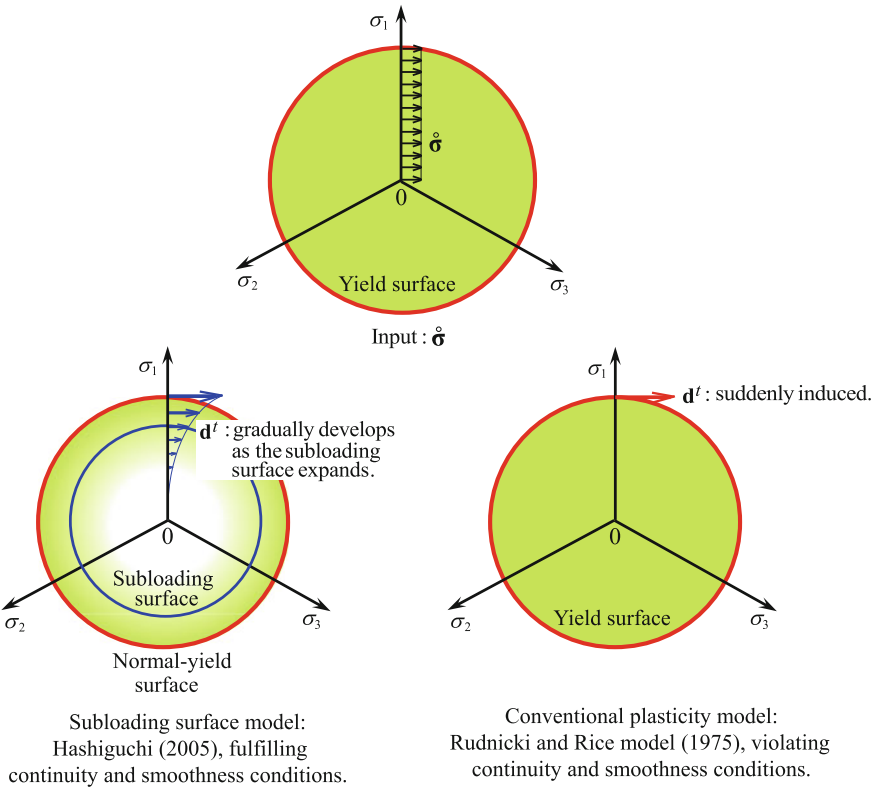

Fig. 7.17 Incorporation of tangential inelastic strain rate illustrated for von Mises yield surface

Equations (7.64) and (7.69) are given for the Hooke's law in Eq. (5.35) as follows:

$$\mathbf{d} = \left(\mathbf{E}^{-1} + \frac{\mathbf{n} \otimes \mathbf{n}}{\bar{M}^p} + \frac{T(R)}{2G} \mathfrak{T}'_t \right) : \mathring{\boldsymbol{\sigma}} \tag{7.70}$$

$$\mathring{\boldsymbol{\sigma}} = \left(\mathbf{E} - \frac{\mathbf{E} : \mathbf{n} \otimes \mathbf{n} : \mathbf{E}}{\bar{M}^p + \mathbf{n} : \mathbf{E} : \mathbf{n}} - 2G \frac{T(R)}{1 + T(R)} \mathfrak{T}'_t \right) : \mathbf{d} \tag{7.71}$$

Here, it is known that the bulk modulus K is irrelevant to the tangential inelastic strain rate which is induced only by the deviatoric part of stress rate.

The loading criterion is given by the equation identical to that without the tangential-inelastic strain rate, since the tangential-inelastic strain rate is always induced by the tangential stress rate.

The tangential-inelastic strain rate $\mathbf{d}^t$ develops gradually as the current stress approaches the normal-yield surface, i.e. the subloading surface expands fulfilling the continuity and the smoothness condition in the subloading surface model as

shown in Fig. 7.17 for the isotropic Mises material. The validity of Eq. (7.70) or (7.71) has been verified by Hashiguchi and Protasov (2004) for metals and Hashiguchi and Tsutsumi (2001, 2003, 2007) and Tsutsumi and Hashiguchi (2005) and for geomaterials. On the other hand, all models other than the subloading surface model violate the smoothness condition. Therefore, they violate also the continuity condition in Eq. (7.1) as illustrated for the J_2-deformation model of Rudnicki and Rice (1975) in Fig. 10. Note that the tangential-inelastic strain rate does not affect the yield surface and thus the consistency condition.

The subloading surface model has been applied to metals (Hashiguchi 1980, 1989; Hashiguchi and Yoshimaru 1995; Hashiguchi and Tsutsumi 2001; Hashiguchi and Protasov 2004; Khojastehpor et al. 2006; Tsutsumi et al. 2006; Hashiguchi et al. 2012) and soils (Hashiguchi and Ueno 1977; Hashiguchi 1978; Topolnicki 1990; Kohgo et al. 1993; Asaoka et al. 1997; Hashiguchi and Chen 1998; Chowdhury et al. 1999; Hashiguchi et al. 2002; Khojastehpor and Hashiguchi 2004a, b; Khojastehpor et al. 2006; Nakai and Hinokio 2004; Hashiguchi and Tsutsumi 2006; Hashiguchi and Mase 2007, 2011; Wongsaroj et al. 2007). Consequently, its capability has been verified widely.

References

Asaoka A, Nakano M, Noda T (1997) Soil-water coupled behaviour of heavily overconsolidated clay near/at critical state. Soils Found 37(1):13–28

Batdorf SB, Budiansky B (1949) A mathematical theory of plasticity based on the concept of slip. NACA TC1871, pp 1–31

Bland DR (1957) The associated flow rule of plasticity. J Mech Phys Solids 6:71–78

Budiansky B (1959) A reassessment of deformation theories of plasticity. J Appl Mech (ASME) 20:259–264

Chowdhury EQ, Nakai T, Tawada M, Yamada S (1999) A model for clay using modified stress under various loading conditions with the application of subloading concept. Soils Found 39 (6):103–116

Christoffersen J, Hutchinson JW (1979) A class of phenomenological corner theories of plasticity. J Mech Phys Solids 27:465–487

Dafalias YF (1985) The plastic spin. J Appl Mech (ASME) 52:865–871

Dafalias YF (1986) Bounding surface plasticity. I: mathematical foundation and hypoplasticity. J Eng Mech (ASCE) 112:966–987

Dafalias YF, Herrmann LR (1980) A bounding surface soil plasticity model. Proc. Int. Symp. Soils Cyclic Trans. Load, Swansea, pp 335–345

Dafalias YF, Popov EP (1975) A model of nonlinearly hardening materials for complex loading. Acta Mech 23:173–192

Dafalias YF, Popov EP (1977) Cyclic loading for materials with a vanishing elastic domain. Nucl Eng Des 41:293–302

Drucker DC (1988) Conventional and unconventional plastic response and representation. Appl Meek Rev (ASME) 41:151–167

Gotoh M (1985) A class of plastic constitutive equations with vertex effect. Int J Solids Struct 21:1101–1163

Goya M, Ito K (1991) An expression of elastic-plastic constitutive laws incorporating vertex formulation and kinematic hardening. J Appl Mech (ASME) 58:617–622

Hashiguchi K (1978) Plastic constitutive equations of granular materials. In: Cowin SC, Satake M (eds) Proceedings of US-Japan seminar on continuum mech stastical approach mechanics granular materials, Sendai, pp 321–329
Hashiguchi K (1980) Constitutive equations of elastoplastic materials with elastic-plastic transition. J Appl Mech (ASME) 47:266–272
Hashiguchi K (1989) Subloading surface model in unconventional plasticity. Int J Solids Struct 25:917–945
Hashiguchi K (1993a) Fundamental requirements and formulation of elastoplastic constitutive equations with tangential plasticity. Int J Plasticity 9:525–549
Hashiguchi K (1993b) Mechanical requirements and structures of cyclic plasticity models. Int J Plasticity 9:721–748
Hashiguchi K (1997) The extended flow rule in plasticity. Int J Plasticity 13:37–58
Hashiguchi K (1998) The tangential plasticity. Met Mater 4:652–656
Hashiguchi K (2000) Fundamentals in constitutive equation: continuity and smoothness conditions and loading criterion. Soils Found 40(3):155–161
Hashiguchi K (2005) Subloading surface model with tangential relaxation. Proc Int Symp Plasticity '05:259–261
Hashiguchi K (2013b) Elastoplasticity theory, lecture note in applied comptational mechanics, 2nd edn. Springer-Verlag, Heidelberg
Hashiguchi K (2016) Exact formulation of subloading surface model: unified constitutive law for irreversible mechanical phenomena in solids. Arch Compt Meth Eng 23:417–447
Hashiguchi K, Chen Z-P (1998) Elastoplastic constitutive equations of soils with the subloading surface and the rotational hardening. Int J Numer Anal Meth Geomech 22:197–227
Hashiguchi K, Mase T (2007) Extended yield condition of soils with tensile strength and rotational hardening. Int J Plasticity 23:1939–1956
Hashiguchi K, Mase T (2011) Physical interpretation and quantitative prediction of cyclic mobility by the subloading surface model. Jpn Geotech J 6:225–241 (in Japanese)
Hashiguchi K, Protasov A (2004) Localized necking analysis by the subloading surface model with tangential-strain rate and anisotropy. Int J Plasticity 20:1909–1930
Hashiguchi K, Tsutsumi S (2001) Elastoplastic constitutive equation with tangential stress rate effect. Int J Plasticity 17:117–145
Hashiguchi K, Tsutsumi S (2003) Shear band formation analysis in soils by the subloading surface model with tangential stress rate effect. Int J Plasticity 19:1651–1677
Hashiguchi K, Tsutsumi S (2006) Gradient plasticity with the tangential subloading surface model and the prediction of shear band thickness of granular materials. Int J Plasticity 22:767–797
Hashiguchi K, Ueno M (1977) Elastoplastic constitutive laws of granular materials, Constitutive equations of soils. In: Murayama S, Schofield AN (eds) Proceedings of 9th international conference soil mechanics and foundation engineering Spec. Ses. vol 9, Tokyo, JSSMFE, pp 73–82
Hashiguchi K, Yoshimaru T (1995) A generalized formulation of the concept of nonhardening region. Int J Plasticity 11:347–365
Hashiguchi K, Saitoh K, Okayasu T, Tsutsumi S (2002) Evaluation of typical conventional and unconventional plasticity models for prediction of softening behavior of soils. Geotechnique 52:561–573
Hashiguchi K, Ueno M, Ozaki T (2012) Elastoplastic model of metals with smooth elastic-plastic transition. Acta Mech 223:985–1013
Hecker SS (1972) Experimental investigation of corners in yield surface. Acta Mech 13:69–86
Hencky H (1924) Zur Theorie plastischer Deformationen und der hierdurch im Material herforgerufenen Nachspannungen. Z A M M 4:323–334
Hill R (1959) Some basic principles in the mechanics of solids without a natural time. J Mech Phys Solids 7:225–229
Hill R (1966) Generalized constitutive relations for incremental deformation of metal crystals. J Mech Phys Solids 14:95–102
Hughes TJR, Shakib F (1986) Pseudo-corner theory: A simple enhancement of J_2-flow theory for applications involving non-proportional loading. Eng Comput 3:116–120

Ikegami K (1979) Experimental plasticity on the anisotropy of metals. Proc Euromech Colloquium 115:201–242
Ito K (1979) New flow rule for elastic-plastic solids based on KBW model with a view to lowering the buckling stress of plates and shells. Tech Report Tohoku Univ 44:199–232
Khojastehpour M, Hashiguchi K (2004a) The plane strain bifurcation analysis of soils by the tangential-subloading surface model. Int J Solids Struct 41:5541–5563
Khojastehpour M, Hashiguchi K (2004b) Axisymmetric bifurcation analysis in soils by the tangential-subloading surface model. J Mech Phys Solids 52:2235–2262
Khojastehpour M, Murakami Y, Hashiguchi K (2006) Antisymmetric bifurcation in a circular cylinder with tangential plasticity. Mech Mater 38:1061–1071
Kohgo Y, Nakano M, Miyazaki T (1993) Verification of the generalized elastoplastic model for unsaturated soils. Soil Found 33(4):64–73
Koiter WT (1953) Stress-strain relations, uniqueness and variational theories for elastic-plastic materials with a singular yield surface. Quart Appl Math 11:350–354
Krieg RD (1975) A practical two surface plasticity theory. J Appl Mech (ASME) 42:641–646
Mandel J (1965) Generalisation de la theorie de plasticite de W.T. Koiter. Int J Solids Struct 1:273–295
Mroz Z (1966) On forms of constitutive laws for elastic-plastic solids. Arch Mech Stos 18:3–35
Mroz Z (1967) On the description of anisotropic workhardening. J Mech Phys Solids 15:163–175
Mroz Z, Norris VA, Zienkiewicz OC (1981) An anisotropic, critical state model for soils subject to cyclic loading. Geotechnique 31:451–469
Nakai T, Hinokio M (2004) A simple elastoplastic model for normally and over consolidated soils with unified material parameters. Soils Found 44(2):53–70
Petryk H (1991) On the second-order work in plasticity. Arch Mech 43:377–397
Petryk H (1997) Plastic instability: criteria and computational approaches. Arch Comput Approach Meth Eng 4:111–151
Petryk H, Thermann K (1997) A yield-vertex modification of two-surface models of metal plasticity Arch Mech 49:847–863
Prager W (1949) Recent development in the mathematical theory of plasticity. J Appl Mech (ASME) 20:235–241
Rudnicki JW, Rice JR (1975) Conditions for the localization of deformation in pressure-sensitive dilatant materials. J Mech Phys Solids 23:371–394
Sewell MJ (1973) A yield-surface comer lowers the buckling stress of an elastic-plastic plate under compression. J Mech Phys Solids 21:19–45
Sewell MJ (1974) A plastic flow at a yield vertex. J Mech Phys Solids 22:469–490
Simo JC (1987) A J_2-flow theory exhibiting a corner-like effect and suitable for large-scale computation. Comput Meth Appl Mech Eng 62:169–194
Topolnicki M (1990) An elasto-plastic suboading surface model for clay with isotropic and kinematic mixed hardening parameters. Soils Found 30(2):103–113
Truesdell C (1955) Hypo-elasticity. J Rational Mech Anal 4:83–133
Tsutsumi S, Hashiguchi K (2005) General non-proportional loading behavior of soils. Int J Plasticity 21:1941–1969
Tsutsumi S, Toyosada M, Hashiguchi K (2006) Extended subloading surface model incorporating elastic limit concept. In: Proceedings of plasticity *'06*, Halifax, pp 217–219
Wang Z-L, Dafalias YF, Shen C-K (1990) Bounding surface hypoplasticity model for sand. J Eng Mech (ASCE) 116:983–1001
Wongsaroj J, Soga K, Mair RJ (2007) Modeling of long-term ground response to tunneling under St James' Park, London. Geotechnique 57:75–90